Egyptian Geophysical Society
EGS Journal, Vol. 17, No. 1, 129-137 (2019)

3D SEISMIC STUDY OF A DETACHMENT PLIOCENE/PLEISTOCENE FAULT SYSTEM IN THE EAST NILE DELTA, EGYPT

M.H. SALEH[(1)], A.R. MOUSTAFA[(2)] and P. BENTHAM[(1)]
(1) British Petroleum Company, BP Egypt.
(2) Geology Department, Faculty of Science, Ain Shams University, Cairo, Egypt.

دراسة البيانات السيزمية ثلاثية الأبعاد لنظام صدوع الانفصال بالبلايوسين و البلايوستيسن في شرق دلتا النيل . مصر

الخلاصة: تتكون الطيات المتزامنة مع الترسيب مع التراكيب المصاحبة لقوى الشد التي يكثر انتشارها في التراكيب الجيولوجية المصاحبة لرواسب المتبخرات و ينظر اليها على أنها تتكون نتيجة انحناء الطبقات الرسوبية على الحائط العلوي للصدوع بالاضافة إلى ازاحة الرواسب إلى أسفل مع الترسيب السريع فوق صدوع الانفصال. ويكون شكل هذه الصدوع مقعرا إلى أعلى في القطاع الراسي ومقعرا أيضا في المسقط الأفقي.

وعندما انفصل البحر المتوسط عن المحيط الاطلنطي خلال فترة المسينيان ترسبت طبقات سميكة من المتبخرات الملحية في حوضه الترسيبي. وقد لعبت هذه الرواسب دورا هاما في تكوين التراكيب الجيولوجية التي أثرت في رواسب عصري البلايوسين و البلايوستوسين في الحوض الترسيبي الشرقي للبحر المتوسط وفيه تظهر صدوع الانفصال التي تتسطح لأسفل على ترسيبات عصر المسينيان مكونة تركيبات معقدة للغاية. وقد استخدمت في هذه الدراسة حزم البيانات السيزمية ثلاثية الأبعاد لتفسير ووصف التراكيب الجيولوجية المصاحبة للطيات على صدوع الانفصال. كما استخدمت ايضا تقنيات تحليل الترددات ومزج اطياف الالوان لاظهار التراكيب المختلفة و مدى تعقيداتها بشكل أفضل. وقد تكونت تلك الطيات على الحوائط العلوية لصدوع الانفصال فى نطاق واسع متخذا الاتجاه شمال غرب . جنوب شرق. واشتملت هذه الدراسة على تخريط الاسطح السيزمية المختلفة في عصور جيولوجية ممتدة من عصر الاوليجوسين إلى قاع سطح البحر.

ABSTRACT: *Rollover anticlines are syn-sedimentary extensional structures that are commonly associated with salt tectonics. They are considered to result from layer bending of hanging wall sides syn-kinematically while displacing sediments with a rapid sedimentary progradation above growth faults. They are commonly listric in cross section and concave to the basin in a plan-view. The Mediterranean was isolated from the Atlantic Ocean during the Messinian time depositing thick layers of evaporites. These Messinian evaporites played an important role in the Pliocene and Pleistocene structures in the eastern Mediterranean basin. Structured growth faults, which detach at the Messinian level, form a complex structural setting.*
In this study three-dimensional seismic data sets were interpreted to describe the structures associated with a rollover anticline. Frequency decomposition and color blending techniques were used to reveal the structures and their complexity in a better way. The anticline formed in the hanging wall blocks of growth faults is a broad rollover, which extends in a NW-SE direction. Interpreted seismic levels cover the stratigraphic section extending from the Oligocene to present-day seabed.

I. INTRODUCTION

The study area is located north of Akhen/Temsah fields, east of Satis discovery and west of Salamat/Atoll discoveries in a complex structural and stratigraphic setting (Figure 1). The area has several transpressional anticlines where multi-Trillion Cubic Feet (TCF) of gas accumulations have been discovered. The Messinian Salinity Crisis (MSC) developed in three main stages, each of them characterized by different palaeo environmental conditions. During the first stage, evaporites precipitated in shallow sub-basins; the MSC peaked in the second stage when evaporite precipitation shifted to the deepest depocentres; the third stage was characterized by large- scale environmental fluctuations, which transformed the Mediterranean into a brackish water lake. The high-resolution timescale available for some Late Miocene intervals in the Mediterranean makes it possible to consider environmental variability on extremely short time scales including, in some places, annual changes (Roveri et al. 2013).

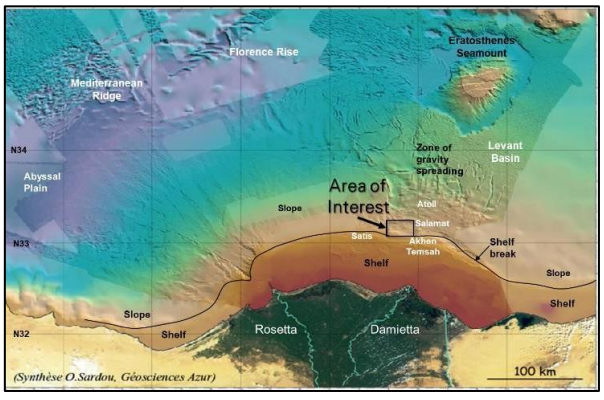

Figure 1: Area of interest on a shaded bathymetric map of the Nile Delta Deep-Sea Fan (modified after loncke et al., 2006).

Pliocene or older Neogene sediments are often covered by Quaternary deposits (such as the coastal ridges constituted by oolitic limestones found along the northern coasts of the Western Desert), Said (1971). The Pliocene transgression deposits are followed by an arid

period that corresponds to the beginning of desertification in Saharan regions. This arid phase is considered the early Pleistocene in Egypt (Paleonile-Protonile interval of Said 1981). This arid sequence is overlain by a sequence of sandstones and conglomerates (Philibbos and Haddad 1984) followed by various raised organic reefs separated by conglomeratic intervals, corresponding to the late Quaternary tectonic activity.

II. DATA AND METHODOLOGY

The area of interest (AOI) is approximately 560 km^2 and is fully covered by a moderate to high-resolution 3D seismic data (Figure 1). The dataset provides good definition of both the hanging wall structure and the bounding faults associated with growth faults. It also highlights the complexity of the structure and stratigraphy within the study area. The 3D seismic data were used for interpretation of both stratigraphy and faults using Petrel software package and were tied to the existing wells.

Faults were interpreted on the 3D seismic data and mapped across the study area. Key stratigraphic horizons were interpreted to delineate the structural complexity and identify key events that took place during deposition. Fourteen different horizons were interpreted; two horizons within the deeper Oligocene/Miocene sections, base and top Messinian, four horizons within the Pliocene section, a Pliocene/Pleistocene boundary level, four horizons within the Pleistocene section, and the seabed.

The horizon interpretation was conducted on a 64x64 mapping grid (in-line and x-line directions). The horizons then went into another level of machine auto-tracking based on the picked character of the seismic data to provide more detail and fill-in the associated gaps within the interpretation with controlled quality. Most of the fault interpretation took place every 10 lines to achieve the required detail. The rest of faults were interpreted every 32 lines. Faults and horizons truncations were then adjusted. Four seismic lines were selected to show the structuration and the complexity in the study area.

Seismic attributes were used within the study area to better define the fault distribution within the area of interest. Both Petrel and GeoTeric software packages were used to generate different attributes. Petrel was used for generating variance cubes, whereas GeoTeric was used for frequency decomposition and color blending techniques.

GeoTeric's Frequency Decomposition Module allows discrete frequency responses to be isolated and combined with Red, Green, Blue (RGB) blending, which utilizes bandpass filters to carry out decomposition. There are multiple methods available to do so, the maintaining good frequency resolution method is the one used in this paper. The Frequency RGB blends reveals geological features in seismic data much more clearly than other attributes. It highlights subtle variations/heterogeneity within a given geological entity and allow differentiation of features with similar amplitude characteristics (Figure 2).

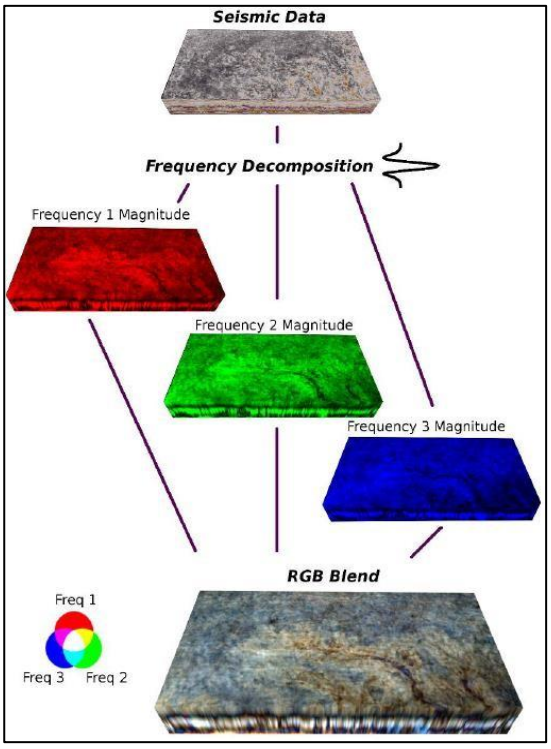

Figure 2: GeoTeric software's schematic frequency decomposition workflow.

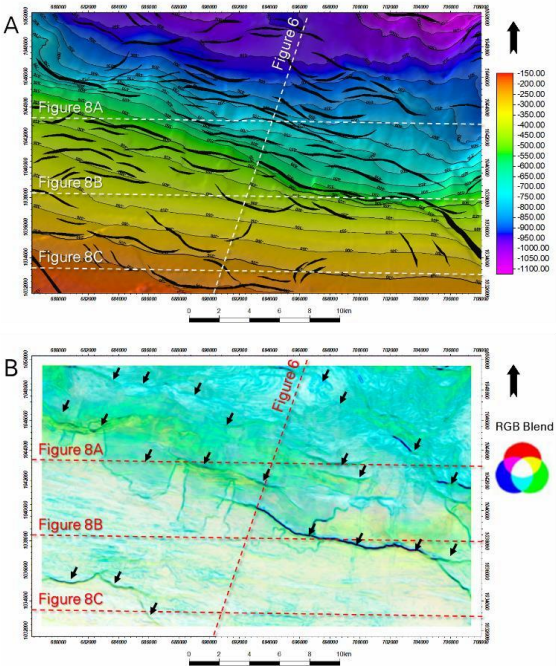

Figure 3: Seabed two-way time structure map. (A) a directional spotlight is applied using Petrel software towards the southeast direction to elaborate the geomorphological variations within the surface as well as the subtle elevation changes. (B) Color blended extraction along the seabed from a frequency decomposed seismic volume using GeoTeric software; black arrows show the present-day active faults at the seabed. Locations of the seismic lines examples shown in this paper are highlighted in dashed lines.

Two levels, Seabed and a Pleistocene surface, are presented in this paper showing the enhancement in fault delineation between the conventional two-way time 3D seismic interpretation and the attributed view of an extracted frequency decomposition values along the 3D interpreted surface (Figure 3 and Figure 4 **Error! Reference source not found.**).

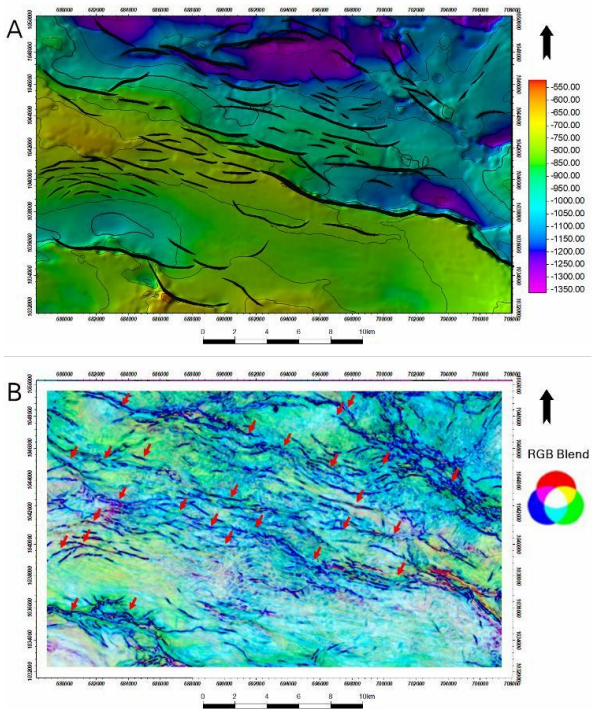

Figure 4: A two-way time structure map at one of the Pleistocene levels. (A) a directional spotlight is applied using Petrel software towards the southeast direction to elaborate the geomorphological variations within the surface as well as the subtle elevation changes. (B) Color blended extraction along the seabed from a frequency decomposed seismic volume using GeoTeric software; red arrows show the effectiveness of such technique for enhancing the visualization of the sub-seismic imaging of the faults.

III.KINEMATICS OF GROWTH FAULTS

The structures associated with the Pliocene-Pleistocene section within the study area are mainly a set of listric growth faults with rollover anticlines. In most cases the growth faults detach at the base of the Messinian level. The Messinian level is mainly composed of salts and anhydrites that act as a perfect detaching surface for the younger, relatively unconsolidated siliciclastic section.

Listric growth faults are characteristic of thin-skinned, gravity-driven deformation in sequences of poorly lithified sediments (Bally et al., 1981, Roberts and Yielding, 1994). In listric growth fault systems, a concave-upward bounding fault with a basal detachment is overlain by a thick 'wedge' of pre- and syn-faulting hanging wall sediments (Shelton, 1984; Figure 5).

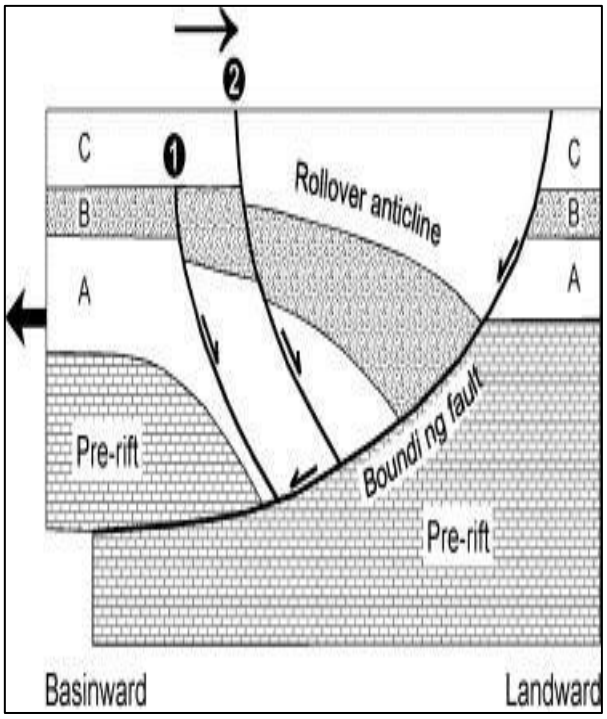

Figure 5: Cartoon summarizing the principal features of listric growth fault systems. Packages of syn-faulting sediments in the hanging wall to the bounding fault (units A, B and C) are deformed by a geometrically-necessary rollover anticline (Imber et al., 2003 after Shelton, 1984).

Sediment thickness varies across the different bounding faults reflecting a period of fault activity during which the deposition of a certain sedimentary sequence took place. Some authors believe the first growth fault (older fault: labeled #1 in

Figure (5) that dips landward is the oldest. Thus, the locus of active hanging wall growth faulting and the rollover hinge appear to have migrated in a landward direction through time, a feature predicted by 2-D sandbox models of listric growth faults (McClay, 1990a, 1990b).

Based on sandbox experiments; the geometry and position of the bounding fault are determined by the footwall block and therefore remains fixed throughout the model run. Deformation in the hanging wall is controlled by the curvature of the rigid footwall block (McClay et al., 1991, McClay, 1996). Given that; some authors suggest that the footwall collapse-where the bounding fault steps back into the previously undeformed footwall block—could be an important mechanism during the growth of listric fault systems (Gibbs, 1984, Vendeville, 1991). The Pliocene-Pleistocene package within the study area is syn-depositional with the fault movements. Rollover anticlines are cut by a set of growth faults that dip landward, hence pronounced sediment thickening is obvious towards the bounding faults.

The sandbox model E44 (McClay, 1990b); has a fixed listric bounding fault that passes down into a gently 'basinward'- dipping detachment (Figure 6). The

detachment is overlain by a deformable hanging wall and sediment (unconsolidated sand) is added to the hanging wall such that the sedimentation rate keeps pace with the fault displacement rate throughout the experiment (McClay, 1996). Within the modelled hanging wall rollover, the basinward limits of sediment thickening in the A to E growth intervals are narrow zones defined by 'landward'- dipping (i.e. antithetic) growth faults 1, 2, 4, 7 and 8, respectively (Figure 6). Thus, the model predicts that the rollover hinge and associated hanging wall growth faults should migrate progressively landward.

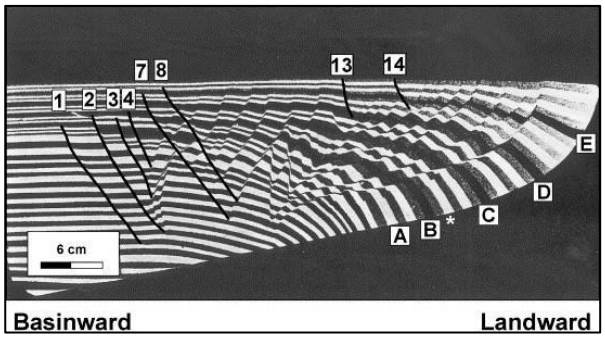

Figure 6: McClay's (1990b) 2-D sandbox experiment E44 at 100% model extension. Regularly spaced markers are pre-rift sediments, alternating wide/narrow markers are syn-rift sediments (labelled A to E). The point at which the curved bounding fault flattens out into a gently 'basinward'-dipping detachment is marked with a star (*).

IV. MAPPING AND INTERPRETATION

The study area has different phases of structuration that took place in sequence. The Pliocene section is decoupled from the Pleistocene section where the different sets of faults per each epoch cut through each other. A broad NW-SE trending anticline is superimposed and tightened up the handing wall rollover anticline associated with the major growth faults. The crest of the anticline is dissected by two sets of conjugate normal faults. These normal faults are associated, in part, with across fault sediment thickness variations while depositing the Pleistocene section (Figure 7).

In an E-W strike direction, sub-parallel to the axial surface of the NW-SE trending anticline, the presence of multiple detaching levels is observed. Three detachment surfaces are noted; one level within the Pliocene section, another one at the boundary between the Pliocene-Pleistocene sections, and the third at Messinian level that is the main detachment affecting all structuration within the study area (Figure 8A)

The seismic data and sections reveal the area is still dynamic with recent motion. At present, the seabed is affected by faulting and gently folded (Figure 7 and Figure 8). The dip seismic sections, trending NE-SW, through the study area show the segmented bounding faults and their associated hanging wall rollover anticline. The anticline is cut by two distinct sets of normal faults: older growth faults that were active, several of them are still active, while depositing the mapped hanging wall sequence, and younger conjugate faults that post-date the deposition of the imaged sequence (Figure 7).

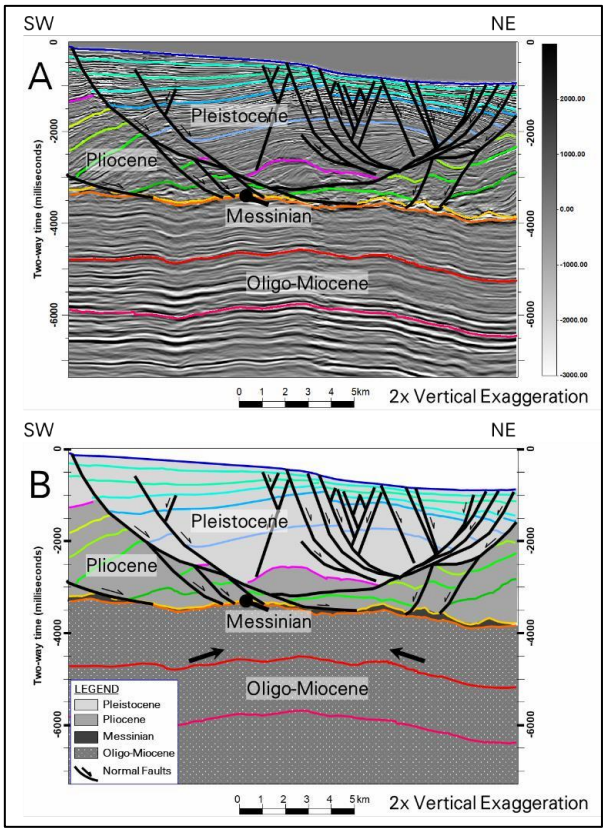

Figure 7: (A) NE-SW trending seismic line interpreted with the different surfaces from Oligocene-Miocene time to the present-day seabed. (B) Cartooned version of the same line. Thick arrows at the Oligocene-Miocene red surfaces show the pre-existing folded structure. See Figure 3 for location.

Figure 8 (A, B and C): E-W Strike seismic lines showing the variation in faults arrangement, detachment levels as well as the different stratigraphic units (Oligocene-Miocene to seabed level). The three sets of seismic lines are presented without and with interpretation as well

The framework structures of the eastern Mediterranean area is complex. It is characterized by an active pattern of thick- skinned, crustal-scale tectonics (McKenzie, 1972, Neev, 1975, Courtillot et al., 1987, Sage and Letouzey, 1990, Le Pichon et al., 1995, Mascle et al., 2000, McClusky et al., 2000), resulting from interactions between various tectonic plates and microplates.

The Egyptian margin, a passive margin of Mesozoic age has been reactivated partly during the Miocene, the timing of rifting the Gulf of Suez and Red Sea (Guiraud and Bosworth, 1999, Mascle et al., 2000). At that time the African and Eurasian plates were subducting towards each other generating a long wave-length folded structures in the pre-Messinian section trending NW-SE direction (e.g. Akhen and Temsah folded structures – See Figure 1).

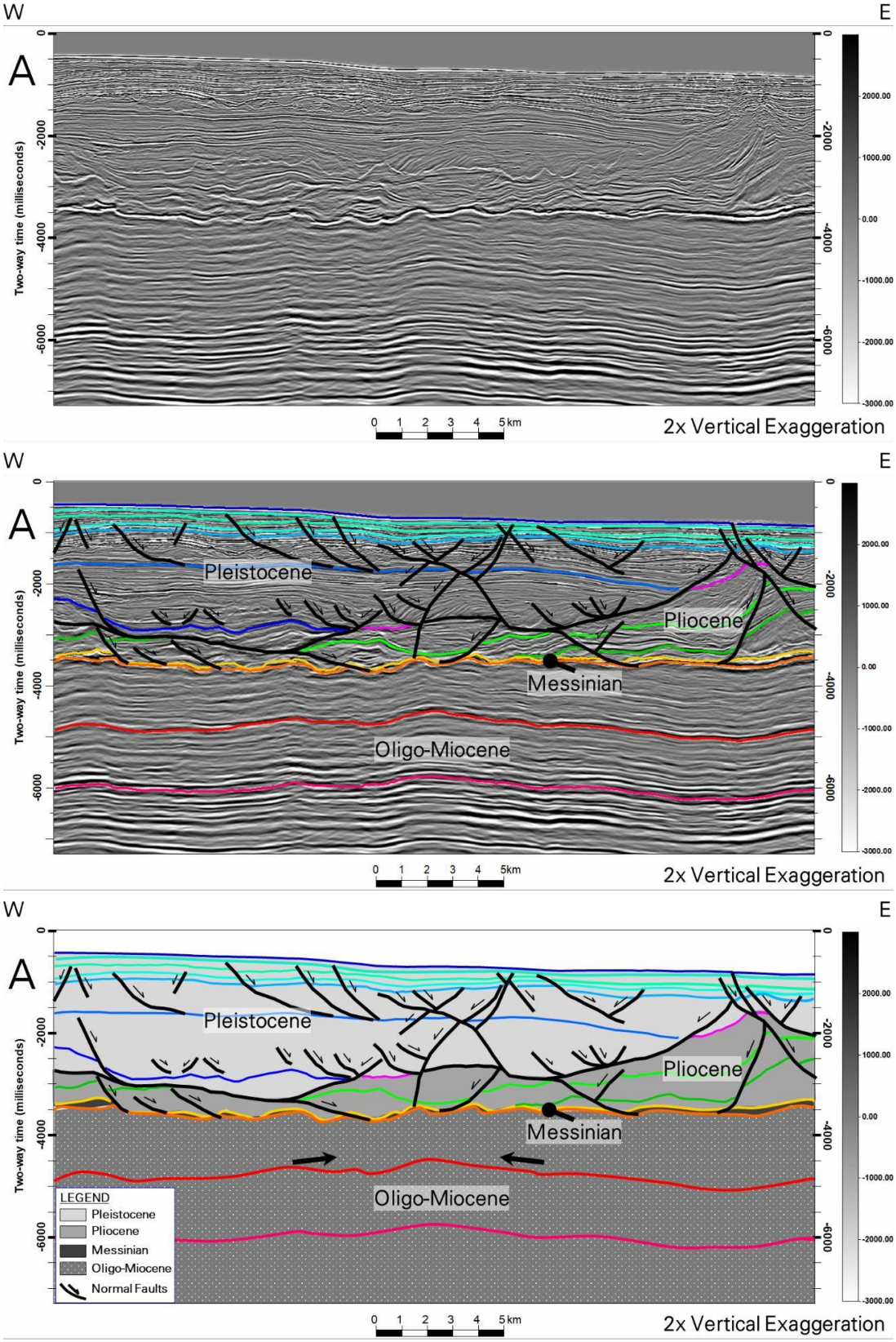

Figure 8 (A, B and C): E-W Strike seismic lines showing the variation in faults arrangement, detachment levels as well as the different stratigraphic units (Oligocene-Miocene to seabed level). The three sets of seismic lines are presented without and with interpretation as well as a cartooned version. See Figure 3 for location. Thick arrows in Figure 8A at the Oligocene-Miocene red surfaces show the pre- existing folded structure.

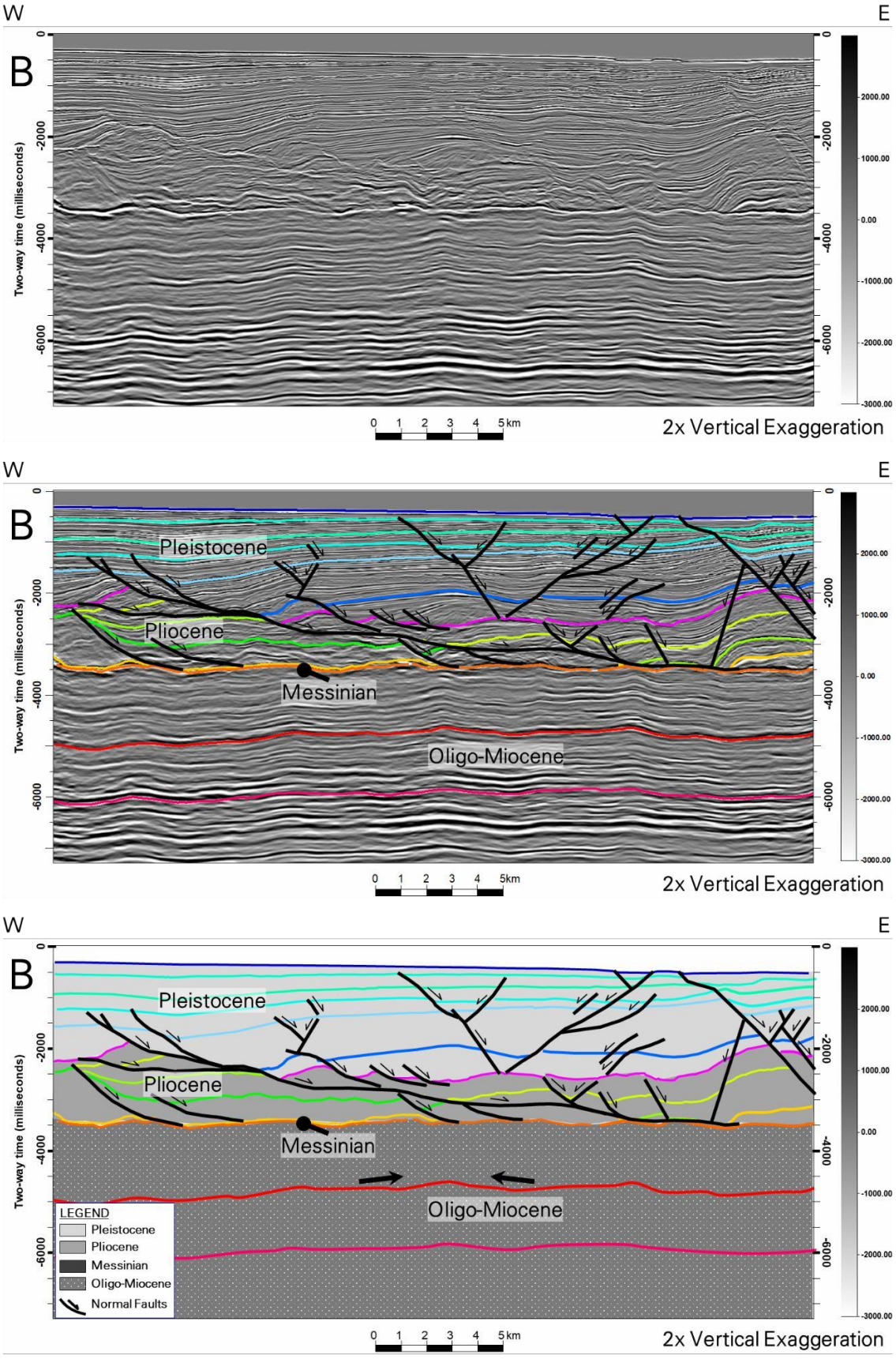

Figure 9B (Continued)

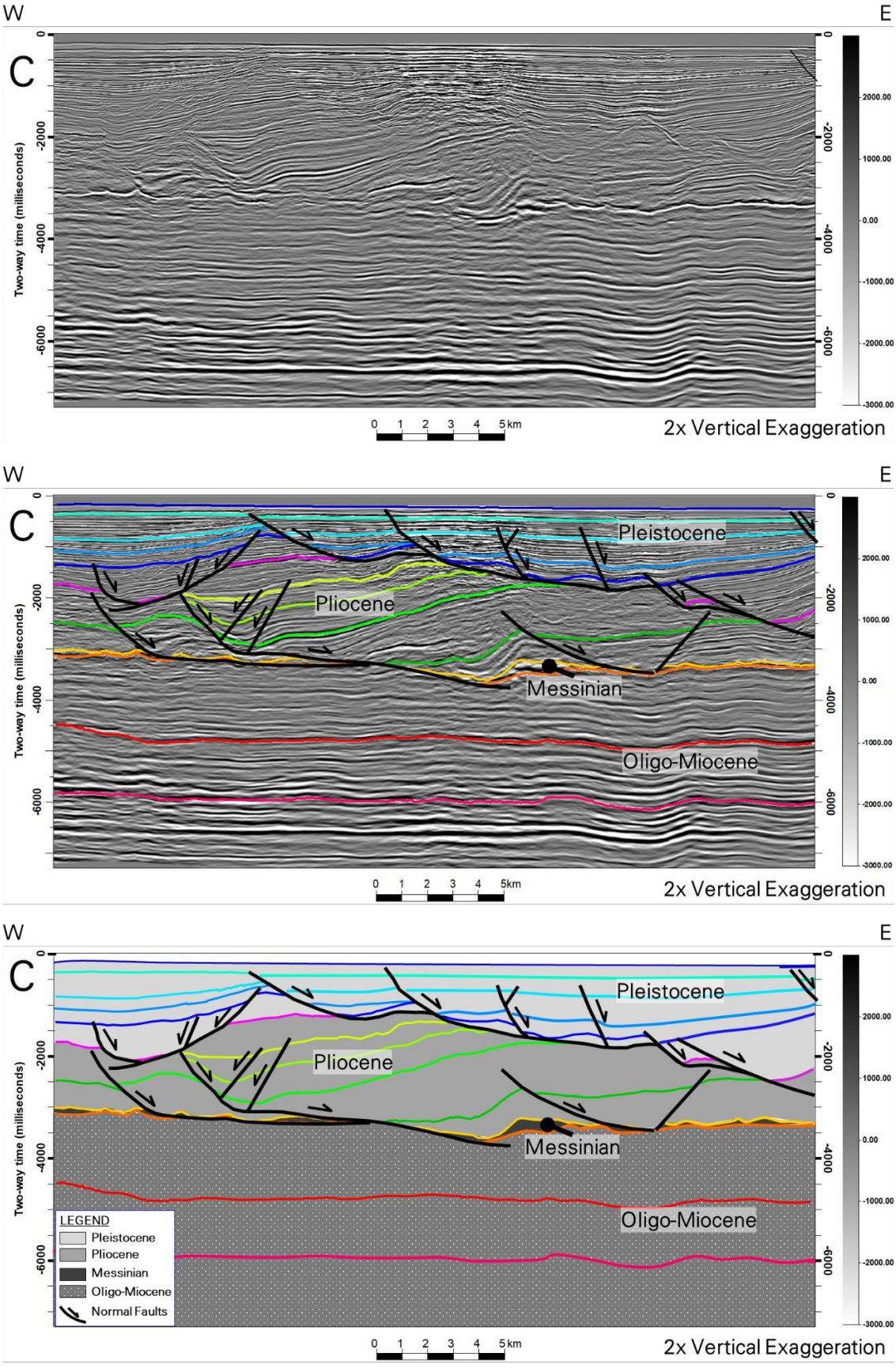

Figure 10C (Continued)

In this study, it is noted that the growth faults over this unstable part of the basin are developed in areas that superimposed the preset fold fabrics in the deeper sections. Hence, a relationship between the pre-existing folded structures (Oligocene-Miocene) and development of growth faults detaching at the Messinian level is present (Figure 7 and Figure 8).

Detailed mapping of faults in the study area has revealed a certain mechanism for fault development. As rollover anticline is formed on the hanging wall of the main growth fault, younger faults are progressively cutting through the footwall block and branch of the main fault along strike as shown in Figure 11. Changes in thickness of the growth stratigraphy has been used to determine the relative age of faults with respect to each other.

CONCLUSION

The salts deposited due to the Messinian Salinity Crisis are the primary cause of structuration within the area of interest. Listric faults detach at the Messinian level whereas some other detachment surfaces are also present. The locations of growth faults are controlled by the pre-existing (pre-Messinian) fold structures formed due to convergence of the African and Eurasian tectonic plates.

The studied rollover anticline is oriented in a NW-SE direction bounded by a set of listric faults dipping basinward. On the hanging wall side, syn-kinematic section, a set of growth faults dipping in a landward direction are noted.

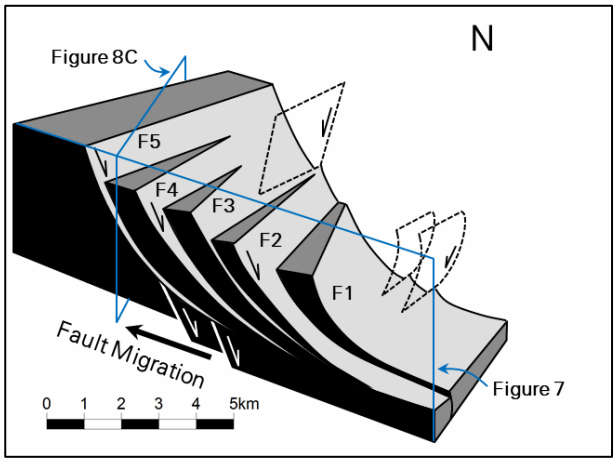

Figure 11: A cartoon for a part of the study area showing the along- strike changes in the structure of the NW-SE trending listric faults together with the locations for some of the presented seismic sections. F1 to F5 are representing the landward-stepping fault segments that make up the bounding fault to the south of the study area.

Detailed mapping and dating of faults have revealed that footwall collapse and back stepping of the first order bounding faults control deformation in the hanging wall and development of thee listric growth fault system in a landward direction (Figure 11).

Seismic attributes and frequency decomposition reveal details enhanced by visualization of the fault distribution within the study area.

ACKNOWLEDGEMENTS

We would like to express our gratitude and appreciation to BP Egypt for allowing us to use its data and publish the results. Mark C. Williams is thanked for his efforts providing constructive review and feedback that improved the manuscript. The first author would like also to thank his family with special thanks to his wife, parents and mother in law for their continuous encouragement and support.

REFERENCES

Bally, A.W., Bernoulli, D. Davis, G.A. Montadert, L., 1981. Listric normal faults. In: Oceanologica Acta: Proceedings of the 26th International Geological Congress: Geology of Continental Margins Symposium, Paris, p. 87-101.

Gennari, R., Manzi, V., Angelettic, L., Bertini, A., Biffi U., Ceregato, A., Faranda, C. Gliozzi, E., Lugli, S., Menichetti, E., Rosso, A., Roveri, M., Taviani, M. 2013. A shallow water record of the onset of the Messinian salinity crisis in the Adriatic foredeep (Legnagnone section, Northern Apennines): Palaeogeography, Palaeoclimatology, Palaeoecology, 386, p. 145-164.

Gibbs, A.D., 1984. Structural evolution of extensional basin margins: Journal of the Geological Society, 141, p. 609-620. Guiraud, R. and Bosworth, W. 1999. Phanerozoic geodynamic evolution of northeastern Africa and the northwestern

Arabian platform: Tectonophysics, 315, p. 73-108.

Imber, J., Childs, C., Nell, P.A.R. Walsh, J.J., Hodgetts, D., Flint, S. 2003. Hanging wall fault kinematics and footwall collapse in listric growth fault systems: Journal of Structural Geology, 25, Issue 2, p. 197-208.

Loncke, L.A., Gaullier, V.B., Mascle, J.C., Vendeville, B. D., Camera L. (2006). The Nile deep-sea fan: An example of interacting sedimentation, salt tectonics, and inherited subsalt paleotopographic features, Nile Delta, Egypt: Marine and Petroleum Geology, 23, p. 297-315.

McClay, K.R., 1990a. Extensional fault systems in sedimentary basins: A Review of analogue model studies: Marine and Petroleum Geology, 7, 206-233.

McClay, K.R., 1990b. Physical models of structural styles during extension. In: Tankard, A.J., Balkwill, H.R. (Eds.), Extensional Tectonics and Stratigraphy of the North Atlantic Margins, Tulsa: AAPG Memoir, 46, p. 95-110.

McClay, K.R., 1996. Recent advances in analogue modelling: uses in section interpretation and validation. In: Buchanan, P.G., Nieuwland, D.A. (Eds.), Modern Developments in Structural Interpretation, Validation and Modelling:

Geological Society Special Publication, 99, p. 201-225.

McClay, K.R., Waltham, D.A. Scott, A.D., Abousetta, A., 1991. Physical and seismic modeling of listric normal fault geometries. In: Roberts, A.M., Yielding, G., Freeman, B. (Eds.), The Geometry of Normal Faults: Geological Society Special Publication, 56, p. 231-239.

Mascle, J., Benkhelil, J., Bellaiche, G. Zitter, T., Woodside, J., Loncke, L. 2000. Marine geologic evidence for a Levantine- Sinai plate, a missing piece of the Mediterranean puzzle: Geology, 228, p. 779-782.

Philobbos, E.R. and El Haddad, A.A. 1983. Contribution to Miocene and Pliocene lithostratigraphy of the Red Sea coastal zone, 21st Annual meeting, Egypt: Geological Society, p. 5-6 (abstract).

Roberts, A., Yielding, G., 1994. Continental extensional tectonics. In: P.L. Hancock (Ed.), Continental Deformation, Pergamon: Oxford, p. 223-250.

Roveri, M., Bassetti, M.A. Lucchi, F.R. 2001. The Mediterranean Messinian salinity crisis: An Apennine foredeep perspective: Sedimentary Geology, 140, 201-214.

Said, R., 1962. The Geology of Egypt, Elsevier, Amsterdam, 377 p.

Said, R., 1981. The Geological Evolution of the River Nile, Springer-Verlag, 151 p.

Shelton, J.W., 1984. Listric normal faults: an illustrated summary: AAPG Bulletin, 68, p. 801-815.

Vendeville, B., 1991. Mechanisms generating normal fault curvature: a review illustrated by physical models. In: Roberts, A.M., Yielding, G., Freeman, B. (Eds.), The Geometry of Normal Faults: Geological Society Special Publication, 56, p. 241-249.